

# An extended Monod-Wyman-Changeaux-model expressed in terms of the Herzfeld-Stanley formalism applied to oxygen and carbonmonoxide binding curves of hemoglobin trout IV

Reinhard Schweitzer-Stenner and Wolfgang Dreybrodt

University of Bremen, FB 1 - Physics Department 2800 Bremen 33, Federal Republic of Germany

**ABSTRACT** An extended Monod, Wyman, Changeaux (MWC)-model, the mathematical basis of which had been formulated by Herzfeld and Stanley (*J. Mol. Biol.* 82:231, 1974.) was used to fit oxygen and CO-binding curves of hemoglobin trout IV measured at different pH-values between pH = 8.0 and

6.0. From this calculation one obtains that even the fully liganded molecule exhibits a R  $\rightarrow$  T quaternary transition upon approaching the acid pH-region. In the case of O<sub>2</sub>-binding, the cooperativity becomes negative below pH = 6.5. This can be related to the difference between the equilibrium con-

stants of proton binding to the  $\alpha$ - and  $\beta$ -subunits. Furthermore, it can be shown that the interaction between the quaternary T  $\rightarrow$  R- and the tertiary t  $\rightarrow$  r-transitions is different for the  $\alpha$ - and  $\beta$ -subunits.

## INTRODUCTION

Hemoglobin from teleost fish exhibits a very marked pH-dependence of its ligand affinity. The effect is associated with both, a shift in the position of the ligand curve (Bohr effect) and a drastic change of the cooperativity (Root effect, cf. Brunori, 1975). In the case of oxygen binding to hemoglobin trout IV (the fourth component of hemoglobin trout) for instance, the cooperativity decreases significantly as pH is lowered (Brunori et al., 1978). At pH = 6.1 the Hill coefficient is  $<1$  thus reflecting negative cooperativity. Furthermore the oxygen binding curves become asymmetric at acid pH-values. In contrast to human HbA, CO-binding to this molecule displays a pH-dependence different from that of oxygen (Wyman et al., 1978). Even though the Hill coefficient decreases when approaching the acid region, negative cooperativity is not achieved. These findings are not in accordance with the pure MWC-model (Monod et al., 1966; Brunori et al., 1978).

Here we present a modified version of an allosteric model suggested by Herzfeld and Stanley (1974) (Herzfeld-Stanley [HS]-model). It combines the concepts of the two state MWC-model of Monod et al. (1966) with the results obtained by x-ray studies on human hemoglobin (Perutz, 1970) showing that subunits can exist in the high affinity r-state even though the molecule is in the quaternary T-state and vice versa. To account for this the model considers allosteric interactions between the quaternary states of the molecule and the tertiary states of each individual subunit (quaternary-tertiary interaction). Furthermore the model considers interactions between the tertiary states of adjacent subunits (nearest neighbor interaction) in accordance with the induced fit model of Koshland et al. (1967).

In order to explain the Bohr effect three types of interactions between the proton- and ligand binding sites are introduced: (a) the direct interaction between the titrable amino acid group and the binding site of the ligand (direct effector), (b) the interaction between the titrable amino acid group and the tertiary state of the respective subunit (tertiary effector), (c) the interaction between the titrable amino acid group and the quaternary state of the molecule (quaternary effector).

Applying the HS-model to oxygen and CO-binding curves, experimentally obtained by Brunori et al. (1978) and Wyman et al. (1978), we calculate the equilibrium constants of all the binding processes and the conformational transitions involved. From these data one finds that the Root effect is mainly due to interactions between quaternary and tertiary structural changes, which are significantly different for the  $\alpha$  and  $\beta$  subunits. Furthermore evidence is provided that the nearest neighbor interaction introduced by Koshland et al., 1966 does not contribute to the allosteric process.

In a subsequent paper we will show that the results of these investigations can be used to explain the pH-dependence of symmetry classified distortions of the prosthetic heme group, which have been obtained by resonance Raman spectroscopy (Schweitzer-Stenner et al., 1989).

## THEORY

In order to describe the basic principles of the HS-model, we first formulate the energy contributions to the unoccupied molecule. This is achieved by starting within the framework of MWC-model, which will then be extended step by step, considering (a) interactions among the

quaternary and tertiary states, (b) interactions among different subunits, and (c) the structural differences among the  $\alpha$ - and  $\beta$ -subunits. The final step of our model deals with the binding of ligands and effectors to respective binding sites of the subunits.

## The energy contributions in the absence of ligands and effectors

### Contributions due to the MWC-model

The MWC-model is based on the following assumptions: (a) The tetrameric hemoglobin molecule can exist in two different quaternary states  $T$  and  $R$ . In the  $T$ -state the molecular conformation is determined by a large number of noncovalent bonds among the subunits (Perutz, 1970). A  $T \rightarrow R$  transition is caused by rupture or weakening of those bonds, thus providing a more relaxed quaternary state. The energies of the  $T$ - and  $R$ -state are written as

$$G_q = qG_q^0, \quad (1)$$

where  $q = 1, 2$  labels the  $T$ - and  $R$ -state respectively.  $G_q^0$  denotes the free energy difference among the  $T$ - and  $R$ -state. Those two quaternary states are displayed schematically in Fig. 1. (b) The subunits containing the active sites of ligand and effector binding can exist in two different tertiary conformations  $r$  and  $t$ . The MWC-model postulates that all subunits exist in the same conformation, either in the  $r$ -state, if the tetramer is in the  $R$ -configuration or in the  $t$ -state, if the quaternary state is  $T$  (cf. Fig. 1). Furthermore it assumes that the ligand binding affinities are different in the  $r$ - and  $t$ -states, respectively.

Analogous to Eq. 1 the energy of the tertiary states is given by

$$g_{\tau_j} = \tau_j g_{\tau_j}^0. \quad (2)$$

$\tau_j = 1, 2$  label the  $t$ - and  $r$ -state of the  $j$ th subunit respectively,  $g_{\tau_j}^0$  denote the free energy difference among two different tertiary states. (c) With respect to the tertiary energy difference  $g_{\tau_j}^0$ , the  $\alpha$ - and  $\beta$ -chains are assumed to be equivalent. Therefore the total energy of the unliganded molecule can be written as

$$G_T^{\text{MWC}} = qG_q^0 + \sum_{\tau_j} \tau_j g_{\tau_j}^0 \delta_{\tau_j q} \quad (3)$$

$\delta_{\tau_j q}$  denotes the Kronecker symbol.

## Extension of MWC-model

### Quaternary-tertiary interaction

Several investigations of the cooperative process of ligand binding in hemoglobin provide evidence that the subunits can exist in the high affinity  $r$ -state even though the molecule is in the quaternary  $T$ -state and vice versa (Perutz, 1970; Szabo and Karplus, 1972).

To account for this a quaternary-tertiary ( $q$ ) interaction has to be introduced, the energy of which is given by:

$$G_{q\tau_j} = -(-1)^{\tau_j+q} G_{q\tau_j}^0, \quad (4)$$

where  $G_{q\tau_j}^0$  provides a convenient zero level.

As one reads from Eq. 4, the  $q\tau$ -interaction energy is positive if  $\tau_j \neq q$ . If the tertiary state is linked to the corresponding quaternary state ( $\tau_j = q$ ), however,  $G_{q\tau_j}$  becomes negative. All configurations possible, are schematically displayed in Fig. 1. It should be noted that  $G_{q\tau_j}^0$  is assumed to be infinite in the MWC-model.

### Inequivalence of the $\alpha$ - and $\beta$ -chains

In contrast to what is assumed in the MWC-model the equivalence of the  $\alpha$ - and  $\beta$ -chains is not in accordance with a larger number of experimental findings (cf. Ten

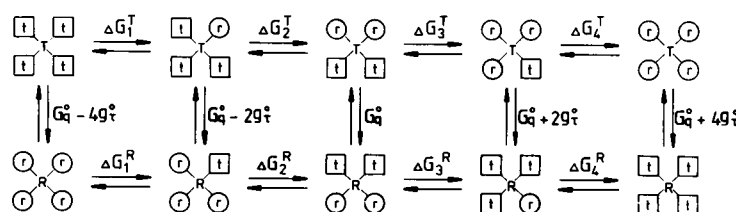


FIGURE 1 Diagrammatic representation of the influence of  $q\tau$ -interaction on the tertiary state of the hemoglobin subunits. ( $r$ :  $r$ -state,  $t$ :  $t$ -state of the subunit).

$$\Delta G_1^T = 2G_{qr}^0 + g_r^0 + 4g_{rr}^0$$

$$\Delta G_2^T = 2G_{qr}^0 + g_r^0$$

$$\Delta G_3^T = 2G_{qr}^0 + g_r^0$$

$$\Delta G_4^T = 2G_{qr}^0 + g_r^0 + 4g_{rr}^0$$

$$\Delta G_5^R = 2G_{qr}^0 - g_r^0 + 4g_{rr}^0$$

$$\Delta G_6^R = 2G_{qr}^0 - g_r^0$$

$$\Delta G_7^R = 2G_{qr}^0 - g_r^0$$

$$\Delta G_8^R = 2G_{qr}^0 - g_r^0 + 4g_{rr}^0.$$

Eyck, 1979; Herzfeld and Stanley, 1974). Therefore each subunit type must be assigned to different energies.

### Nearest neighbor interactions ( $\tau\tau$ -interactions)

The MWC-model completely neglects that conformational changes in one subunit induce variations in the adjacent subunits. Contrary the induced fit model of Koshland et al. (1966) is based entirely on an evaluation of this kind of interaction. It is reasonable to assume that a general model of cooperativity must also consider the interactions among adjacent subunits. The corresponding energy is given by

$$g_{\tau_j\tau_{j+1}} = (-1)^{(\tau_j+\tau_{j+1})} g_{\tau_j\tau_{j+1}}^0 \quad (5)$$

$g_{\tau_j\tau_{j+1}}^0$  defines the zero energy level.

The influence of the  $\tau\tau$ -interaction is considered in Fig. 2. It provides negative contributions to both, the  $\{4r\}$  and the  $\{4t\}$  conformations independent on the actual quaternary state. Mixed configurations as  $\{t, 3r\}$ ;  $\{r, 3t\}$ ; etc.), however, provide positive energy.

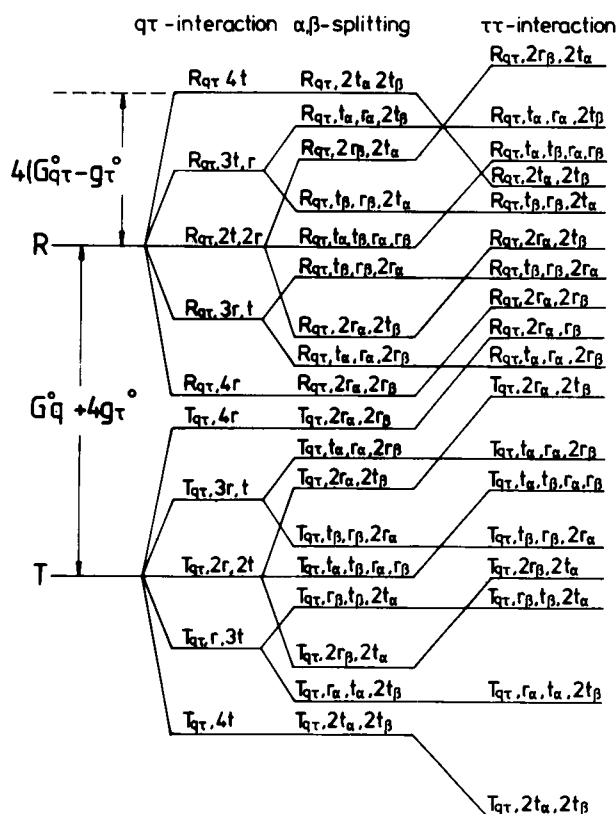


FIGURE 2 Energy level diagram of the unliganded hemoglobin molecule. The respective conformations are denoted by  $Q_q, \nu_j$ , where  $Q_q = R, T$  labels the quaternary state in the presence of  $q\tau$ -interaction and  $\nu_j$  ( $\nu = r, t; j = \alpha, \beta$ ) label the corresponding tertiary states.

By adding Eqs. 1–5 one obtains the total energy of the unliganded molecule as follows:

$$G_c = \sum_q \left\{ qG_q^0 + \sum_{\tau_\alpha} (\tau_\alpha g_{\tau_\alpha}^0 - (-1)^{\tau_\alpha+q} G_{q\tau_\alpha}^0) + \sum_{\tau_\beta} (\tau_\beta g_{\tau_\beta}^0 - (-1)^{\tau_\beta+q} G_{q\tau_\beta}^0) - \sum_{\tau_j\tau_{j+1}} (-1)^{\tau_j+\tau_{j+1}} g_{\tau_j\tau_{j+1}}^0 \right\} \quad (6)$$

The different conformational states resulting from the distinct interactions are visualized by the energy level diagram in Fig. 2, which introduces the different interactions subsequently. Thus, one learns that the  $q\tau$ -interaction splits the  $R$  and  $T$  energy levels into five sublevels. The inequivalence of the  $\alpha$ - and  $\beta$ -subunits causes a further splitting of the states due to the mixed configurations (i.e.,  $\{3r, t\}$ ;  $\{r, 3t\}$ ;  $\{2r, 2t\}$ ) into two separated states. The nearest neighbour interaction, however, in contrast shifts the energy of some configurations without causing further splittings.

It should be noted that for practical purpose only  $\alpha$ - $\beta$ -contacts are considered to contribute to the  $\tau\tau$ -interactions (cf., Ten Eyck, 1979).

### The energy contribution by ligand binding

Considering that the distinct subunits may bind the ligand with different affinities, the change of energy upon ligation can be written as

$$G_{lig} = \sum_\alpha n_\alpha (G_\alpha^0 + (-1)^{\tau_\alpha} G_{L\alpha}) + \sum_\beta n_\beta [G_\beta^0 + (-1)^{\tau_\beta} G_{L\beta}] \quad (7)$$

where  $n_\alpha, n_\beta = 0, 1$  denote the occupation number of the  $\alpha$ - and  $\beta$ -subunits, respectively.  $G_{L\alpha}, G_{L\beta}$  represent half of the energy difference among the liganded  $r$ - and  $t$ -subunits and  $G_\alpha^0, G_\beta^0$  denote the corresponding ligand binding to the subunits, without considering their tertiary conformation.

As one reads from Eq. 7,  $G_{lig}$  becomes positive (high affinity), if  $\tau_\alpha, \tau_\beta$  are equal to two, but is negative (low affinity) if  $\tau_\alpha, \tau_\beta$  are equal to one. Therefore, the total affinity of the tetramer increases with increasing occupation numbers of the  $r$ -states. This is achieved by  $q\tau$ - and by  $\tau\tau$ -interactions.

Fig. 3 illustrates this on one possible example. The energy difference between the unliganded and the fully liganded  $\{T, 4t\}$  conformation is  $2G_\alpha^0 + 2G_\beta^0 - 2G_{L\alpha} - 2G_{L\beta}$ . For simplicity in Fig. 3 we have used  $G_\alpha^0 = G_\beta^0 = G^0$  and  $G_{L\alpha} = G_{L\beta} = G_L$ . Conversion of one subunit from  $t$  to  $r$  in the quaternary  $T$ -state requires some energy because of the  $q\tau$  and  $\tau\tau$ -interactions but causes an increase of the

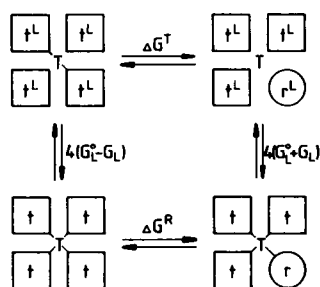


FIGURE 3 Diagrammatic representation of the influence of ligand binding on the tertiary state ( $t^L$ ,  $r^L$  denote the ligated subunits).

ligand affinity by providing a free energy contribution of  $2G_L$ .  $\Delta G^T$  and  $\Delta G^R$  denote the sum of these energies.

### Influence of the effector binding

In order to account for both the Root effect (pH-dependence of the Hill coefficient) and the Bohr effect (pH-dependence of the  $t \rightarrow r$  transitions), we have to consider that binding of a proton to a distinct amino acid side chain can influence both, the tertiary and the quaternary structure. The corresponding energies can be described by:

$$G_e^q = \sum_i n_i [G_{e_i}^{q,0} + (-1)^q G_{e_i}^q] \quad (8a)$$

$$G_e^r = \sum_j \sum_k n_{jk} [G_{e_{jk}}^{r,0} + (-1)^j G_{e_{jk}}^r] \quad (8b)$$

for quaternary and tertiary effector binding, respectively. The occupation numbers of the  $l$ th quaternary effector binding site and the  $k$ th tertiary effector binding site in

the  $j$ th subunit are denoted by  $n_l$  and  $n_{jk}$ , which both can take the values 0, 1, respectively.

The influence of the effector binding on the ligand affinity is visualized in the example depicted by Fig. 4. The energy between the unliganded  $\{T, 4t\}$ - and the fully liganded  $\{R, 4r\}$ -state is lowered by both, the tertiary and the quaternary effector, thus decreasing ligand affinity. This is in general accordance with the observed decrease of  $O_2$ - and  $CO$ -affinity at acid pH-values.

### Calculation of the grand partition sum

In order to describe the ligand binding to the hemoglobin molecule, we consider the system of the protein solution to be in contact with a reservoir of oxygen and effector molecules. Both exchange ligand particles and energy.

The saturation function  $Y$  of the ligand  $L$  can be expressed (Wyman, 1967) as follows:

$$y = \frac{\partial Z}{\partial \mu_L / RT} / 4Z, \quad (9)$$

where  $Z$  denotes the grand partition sum given by

$$Z = \sum_{\text{all states}} \exp \{ [n\mu_L + N\mu_p - G_T] / RT \} \quad (10)$$

$n$  is the number of binding sites occupied in each state,  $N$  is the total number of binding sites of that state,  $\mu_L$  is the chemical potential of the ligand,  $\mu_p$  is the chemical potential of the unoccupied protein.

It should be noted that these chemical potentials  $\mu_L$  and  $\mu_p$  are related to the mole fractions  $X_L$  and  $X_p$  of the ligand

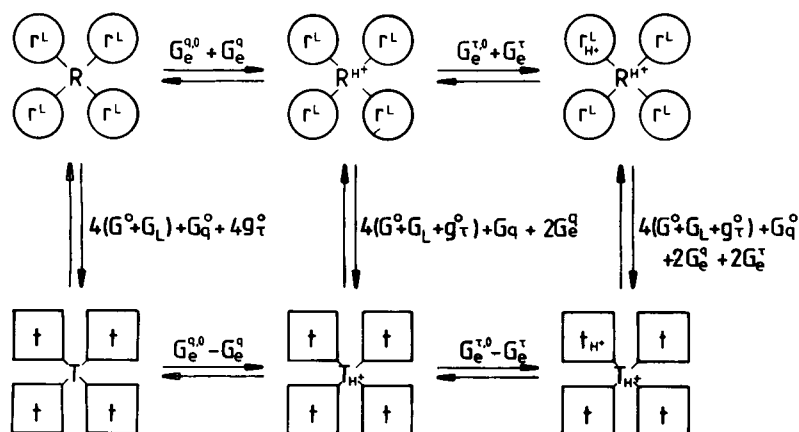


FIGURE 4 Diagrammatic representation of the energy contribution caused by quaternary and tertiary effector proton binding ( $R^{H+}$ ,  $T^{H+}$  denote the quaternary states the energies of which have changed by proton binding,  $r^{H+}$ ,  $t^{H+}$  denote the subunit states influenced by proton binding).

and the protein by

$$\begin{aligned}\mu_L &= RT \ln X_L + \mu_L^0 \\ \mu_p &= RT \ln X_p + \mu_p^0,\end{aligned}\quad (11)$$

where  $\mu_L^0$  and  $\mu_p^0$  denote the standard chemical potentials. Hence the Gibbs-factors and consequently the grand partition sum depend on the ligand concentration.

The total energy can be expressed by considering Eqs. 1–7. This leads to the following expression for the grand partition sum:

$$\begin{aligned}Z &= \sum_{q=1} \left[ \sum_{\tau_1} \cdots \sum_{\tau_2} \exp \left\{ - \left[ qG_q^0 + \sum_{\alpha} \tau_{\alpha} g_{\tau_{\alpha}}^0 + \sum_{\beta} \tau_{\beta} g_{\tau_{\beta}}^0 \right. \right. \right. \\ &\quad \left. \left. - \sum_{\alpha} (-1)^{\tau_{\alpha}+q} G_{q\tau_{\alpha}}^0 - \sum_{\beta} (-1)^{\tau_{\beta}+q} G_{q\tau_{\beta}}^0 \right. \right. \\ &\quad \left. \left. - \sum_j (-1)^{\tau_j+\tau_{j+1}} g_{\tau_j\tau_{j+1}}^0 \right] / RT \right\} \\ &\quad \times \exp (4\mu_p/RT) \\ &\quad \times \sum_{n_4} \cdots \sum_{m_4} \left\{ \exp \left[ - \sum_{\alpha} m_2 (G_{\alpha}^0 + (-1)^{\tau_{\alpha}} G_{L\alpha}) \right. \right. \\ &\quad \left. \left. - \sum_{\beta} n_{\beta} (G_{\beta}^0 + (-1)^{\tau_{\beta}} G_{L\beta}) \right] \right\} \Bigg].\end{aligned}\quad (12)$$

In order to describe the influence of proton binding on the equilibrium between the respective quaternary and tertiary states, we substitute the energies  $G_{\alpha}^0$ ,  $G_{\beta}^0$ , and  $G_q^0$  by corresponding effective energies  $\hat{G}_{\alpha}^0$ ,  $\hat{G}_{\beta}^0$ , and  $\hat{G}_q^0$ , depending on the pH-value of the solution and the equilibrium constants of proton binding. They are calculated by Herzfeld and Stanley (1974) as follows:

$$\begin{aligned}\hat{G}_q^0(\text{pH}) &= G_q^0 \\ &+ \sum_i \ln \left\{ \frac{(1 + \exp [ -(-\mu_H + G_{e_i}^{q,0} + G_{\alpha}^0)/RT ])}{(1 + \exp [ -(-\mu_H + G_{e_i}^{q,0} - G_{\alpha}^0)/RT ])} \right\}\end{aligned}\quad (13a)$$

$$\begin{aligned}\hat{G}_j^0(\text{pH}) &= G_j^0 \\ &+ \sum_k \ln \left\{ \frac{(1 + \exp [ -(-\mu_H + G_{j,k}^{r,0} + G_{\beta}^0)/RT ])}{(1 + \exp [ -(-\mu_H + G_{j,k}^{r,0} - G_{\beta}^0)/RT ])} \right\},\end{aligned}\quad (13b)$$

where  $\mu_H$  is related to the proton concentration  $X^{H^+}$  by

$$\mu_H = RT \ln X^{H^+} + \mu_H^0.\quad (13c)$$

$\mu_H^0$  = standard chemical potential.

To carry out the summations in Eq. 12, Herzfeld and Stanley have applied the following procedure:  $z$  can be composed into two parts

$$Z = Z_q + Z_r,\quad (14)$$

where

$$\begin{aligned}Z_q &= \sum_q \exp \{ -q\hat{G}_q^0(\text{pH})/RT \} \exp \{ 4\mu_L/RT \} \\ Z_r &= \sum_{\tau_1} \cdots \sum_{\tau_2} \prod_q A_q(\tau_j, \tau_{j+1})\end{aligned}\quad (15)$$

The transfer matrix  $A_q$  can be obtained by using the equation:

$$\begin{aligned}A_q(\tau_j, \tau_{j+1}) &= \sqrt{Z_L(\tau_j) Z_L(\tau_{j+1})} \\ &\times \exp \{ - [ \frac{1}{2}(\tau_j g_{\tau_j}^0 + \tau_{j+1} g_{\tau_{j+1}}^0) \\ &\quad - \frac{1}{2}((-1)^{\tau_j+q} G_{q\tau_j}^0 + (-1)^{\tau_{j+1}+q} G_{q\tau_{j+1}}^0) \\ &\quad - (-1)^{\tau_j+\tau_{j+1}} g_{\tau_j\tau_{j+1}}^0 ] / RT \}.\end{aligned}\quad (16)$$

$Z_L(\tau_j)$  is related to the ligation process only. It is written as

$$Z_L(\tau_j) = \sum_{n_j} \{ \exp [ -n_j (G_j^0 + (-1)^{\tau_j} G_{Lj}) / RT ] \}.\quad (17)$$

The transfer matrix  $A_q$  provides a full description of the intrinsic energy for each dimeric  $\alpha\beta$ -configuration of the tetrameric molecule.

Because of the nonequivalence of the  $\alpha$ - and  $\beta$ -subunits,  $\hat{A}_q$  is not a symmetric matrix. It can be decomposed, however, into a symmetric and an antisymmetric part. This leads to

$$\hat{A}_q = \hat{A}_q^s + \hat{A}_q^a,\quad (18)$$

where  $s$  and  $a$  label the symmetric and antisymmetric contributions, respectively.

$\hat{A}_q^s(\tau_j, \tau_{j+1})$  are treated as shown by Herzfeld and Stanley (1974). This yields the following part of the grand partition sum:

$$Z_{\dagger}^s(q) = \sum_j [x_j^s(q)]^4,\quad (19)$$

where  $x_j^s(q)$  is the  $j$ th eigenvalue of  $\hat{A}_q^s$  defined by the secular equation

$$|\hat{A}_q^s - x^s(q)I| = 0.\quad (20)$$

The antisymmetric parts are calculated as follows: One finds that

$$\hat{A}_q^a(\tau_j, \tau_{j+1}) = \hat{A}_q^{aT}(\tau_{j+1}, \tau_{j+2}),\quad (21)$$

where  $\hat{A}_q^{aT}$  denotes the transposed matrix.

Taking this into account one obtains for  $Z_{\dagger}^a(q)$ :

$$Z_{\dagger}^a(q) = \sum_j x_j^a(q),\quad (22)$$

where

$$x_j^a = T_r(\hat{A}_q^a \hat{A}_q^{aT})^2.\quad (23)$$

Using Eqs. 11–13, Eqs. 17 and 18 one obtains the final form of the grand partition sum, which is given by

$$\begin{aligned}Z &= \sum_q \exp \{ -qG_q^0/RT \} \exp \{ 4\mu_p/RT \} \\ &\times \left[ \sum_j (x_j^s(q))^4 + \sum_j x_j^a(q) \right].\end{aligned}\quad (24)$$

Eq. 24 can be inserted into Eq. 8 in order to calculate the partial saturation function  $Y$  in dependence on the ligand concentration and the pH-value of the solution. To relate our final formalism explicitly to these quantities, the following substitutions, which relate chemical potentials to the corresponding mass action constants (Herzberg and Stanley, 1974), have been inserted into Eqs. 12 and 13:

$$P_L K_{ij}^L = \exp \{ -[\mu_L + G_j^0 - G_{ij}^0]/RT \} \quad (25)$$

$$P_L K_{ij}^L = \exp \{ -[-\mu_L + G_j^0 + G_{ij}^0]/RT \} \quad (26)$$

$$[H^+] K_{jk}^H = \exp \{ -[-\mu_H + G_{jk}^{\tau_{j0}} - G_{jk}^{\tau_j}]/RT \} \quad (27)$$

$$[H^+] K_{jk}^H = \exp \{ -[-\mu_H + G_{jk}^{\tau_{j0}} + G_{jk}^{\tau_j}]/RT \} \quad (28)$$

$$[H^+] K_{li}^H = \exp \{ -[-\mu_H + G_{li}^{q_0} - G_{li}^q]/RT \} \quad (29)$$

$$[H^+] K_{li}^H = \exp \{ -[-\mu_H + G_{li}^{q_0} + G_{li}^q]/RT \}. \quad (30)$$

In the following  $L$  stands for  $O_2$  or  $CO$  as ligand and  $P_L$  denotes the partial pressure of the atmosphere in contact to the solution.  $[H^+]$  denotes the hydrogen ion concentrations.

The equilibrium constants are due to the following reactions:  $K_{ij}^L$ ,  $K_{ij}^L$ : equilibrium constants of the ligand binding to the  $j$ -subunit in the  $t$  and  $r$  state, respectively;  $K_{jk}^H$ ,  $K_{jk}^H$ : equilibrium constants of proton binding to the  $k$ th binding site in the  $j$ th subunit either in the  $t$  and  $r$  tertiary conformation;  $K_{li}^H$ ,  $K_{li}^H$ : equilibrium constants of proton binding to the  $l$ th binding site, related to the quaternary  $T$ - and  $R$ -state (quaternary effector).

Eqs. 23–30 now represent the basis for the fitting procedure. Table 1 lists the free parameters used in this procedure. For the computer fit we employed a program called MINUITL from the CERN-library. A detailed description of it has been given elsewhere (James, 1975).

## RESULTS

The theoretical model outlined in the last section has been applied to a set of oxygen binding curves of hemoglobin obtained at  $T = 14^\circ$  by Brunori et al. (1978). As shown in Fig. 5 these curves cover the pH-region between 8.0 and 6.1. The fitting parameters used in the calculation of these curves are given in Table 1. They include pK-values of the tertiary proton binding for the different subunits in the ligated and unligated subunits, and also the pK-values of the quaternary proton binding in the  $R$ - and  $T$ -states. It is obvious that a fitting procedure based on such a large number of free parameters as listed in Table 1 may produce ambiguous results, because correlation effects can occur among distinct parameters. In order to avoid these fundamental difficulties, the following protocol has been adopted for the fitting procedure: (a) We have

TABLE 1 Free parameters used in the fitting procedure

Equilibrium constants of ligand binding	
$K_{t,\alpha\beta}^L$	Equilibrium constant of ligand binding to the $\alpha$ - and $\beta$ -subunits in the tertiary $t$ -state.
$K_{r,\alpha\beta}^L$	Equilibrium constant of ligand binding to the $\alpha$ - and $\beta$ -subunits in the tertiary $r$ -state, $L$ refers to the ligand.
pK-values of Bohr groups	
$pK_{t\alpha 1}$ $pK_{r\alpha 2}$ $pK_{t\beta 1}$ $pK_{t\beta 2}$ $pK_{r\alpha 1}$ $pK_{r\alpha 2}$ $pK_{r\beta 1}$ $pK_{r\beta 2}$	pK-values of the tertiary effector binding sites of the $\alpha$ - and $\beta$ -subunits in the unliganded, low affinity state ( $t$ ) and the liganded, high affinity state ( $r$ ).
pK-values of Root groups	
$pK_{T_1}$ $pK_{T_2}$ $pK_{R_1}$ $pK_{R_2}$	pK-values of the quaternary proton effector binding sites in $T$ - and $R$ -states.
Conformational energies of the unliganded state	
$g_{\tau\alpha\beta}^0$	Energy difference among the $r$ - and $t$ -states of the $\alpha$ - and $\beta$ -subunits, respectively.
$G_{q\tau\alpha\beta}^0$	Energy of the quaternary-tertiary ( $q\tau$ )-interaction.
$g_{\tau\tau j+1}^0$	Energy of the nearest neighbour ( $\tau\tau$ )-interaction.
$G_q^0$	Energy difference among the $R$ - and $T$ -states.

started the analysis assuming that the  $\tau\tau$ -interaction is equal to zero and that both oxygen affinity and the  $q\tau$ -interaction energy are identical for the  $\alpha$ - and  $\beta$ -subunits. ( $g_{\tau\tau j+1}^0 = 0$ ,  $G_{q\tau\alpha\beta}^0 = G_{q\tau\beta\alpha}^0 \neq 0$ ,  $K_{\tau\alpha}^{0_2} = K_{\tau\beta}^{0_2}$ ). As it is depicted in Fig. 5 *a*, the corresponding fit does not agree with the experimental results, even though the loss of cooperativity could be simulated. (b) The second step included  $\tau\tau$ -interaction and different binding constants for the two subunit types. The  $q\tau$ -interaction is assumed to be zero ( $g_{\tau\tau j+1}^0 \neq 0$ ,  $G_{q\tau\alpha\beta}^0 = 0$ ,  $K_{\tau\alpha}^{0_2} \neq K_{\tau\beta}^{0_2}$ ). Hence our model becomes equivalent with the theory of Koshland et al. (1968). As one can read from Fig. 5 *b*, a significantly better fit is achieved. Systematic deviations of the fit from the binding curves measured at pH = 7.7, and 7.1, however, are still evident. Furthermore, unreasonable large differences among  $K_{\tau\alpha}^{0_2}$  and  $K_{\tau\beta}^{0_2}$  have been obtained. (c) As a possible alternative we considered  $q\tau$ -interaction and a difference among  $K_{\tau\alpha}^{0_2}$  and  $K_{\tau\beta}^{0_2}$  ( $G_{q\tau}^0 \neq 0$ ,  $g_{\tau\tau j+1}^0 = 0$ ,  $K_{\tau\alpha}^{0_2} \neq K_{\tau\beta}^{0_2}$ ). The result of the fitting procedure is displayed in Fig. 5 *c*. Satisfactory agreement with the experimental data is now achieved. The obtained values for the free parameters, however, are partially unreasonable. The difference among  $K_{\tau\alpha}^{0_2}$  and  $K_{\tau\beta}^{0_2}$  again is too large. Furthermore an inverse Bohr effect (uptake of protons upon oxygen binding) has to be assumed, which has not been obtained experimentally (Brunori, 1975). (d) An excellent fit and reasonable parameter values have finally been obtained by considering that the  $q\tau$ -interactions are dif-

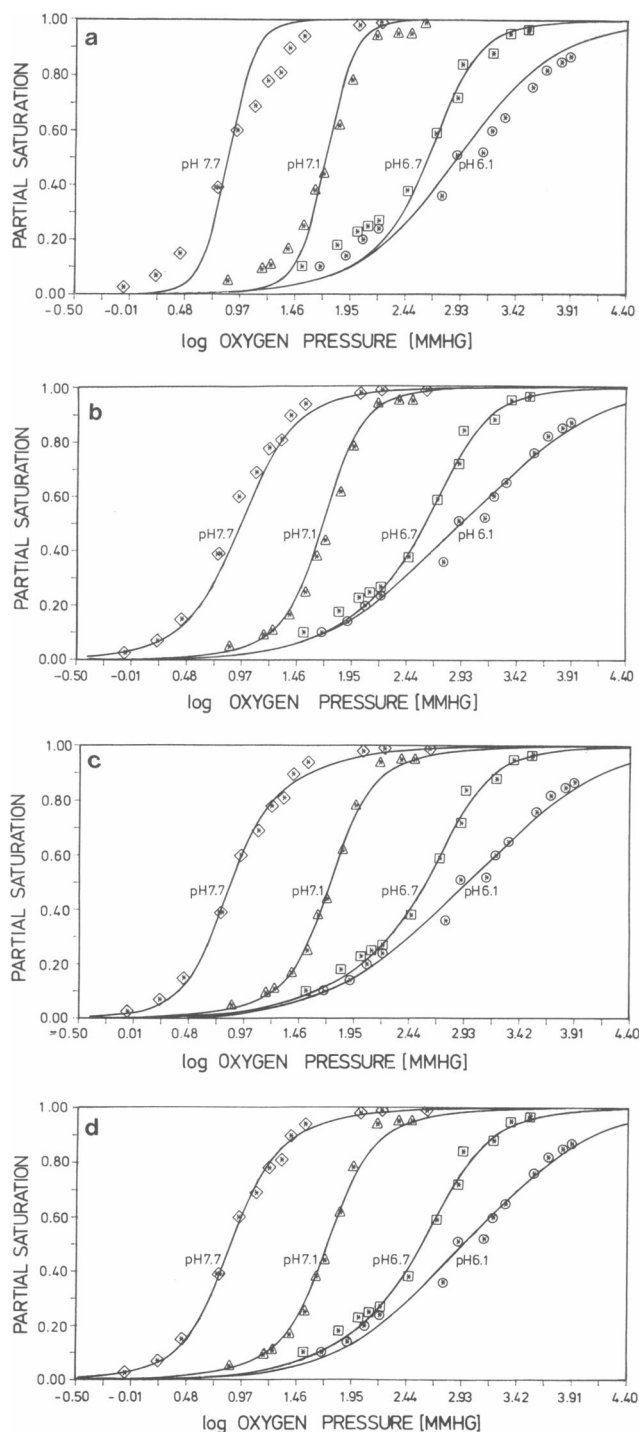


FIGURE 5 Fits to the oxygen binding curves of Brunori et al. (1978).

- (a) For  $G_{\alpha\alpha}^0 = G_{\alpha\beta}^0 \neq 0$ ,  $g_{\tau\tau}^0 = 0$ ,  $K_{\alpha\alpha}^{\text{O}_2} = K_{\alpha\beta}^{\text{O}_2}$ .  
 (b) For  $G_{\alpha\alpha}^0 = G_{\alpha\beta}^0 = 0$ ,  $g_{\tau\tau}^0 \neq 0$ ,  $K_{\alpha\alpha}^{\text{O}_2} \neq K_{\alpha\beta}^{\text{O}_2}$ .  
 (c) For  $G_{\alpha\alpha}^0 = G_{\alpha\beta}^0 \neq 0$ ,  $g_{\tau\tau}^0 = 0$ ,  $K_{\alpha\alpha}^{\text{O}_2} \neq K_{\alpha\beta}^{\text{O}_2}$ .  
 (d) For  $G_{\alpha\alpha}^0 \neq G_{\alpha\beta}^0 \neq 0$ ,  $g_{\tau\tau}^0 = 0$ ,  $K_{\alpha\alpha}^{\text{O}_2} = K_{\alpha\beta}^{\text{O}_2}$ .

ferent for the  $\alpha$ - and  $\beta$ -subunits ( $G_{\alpha\alpha}^0 \neq G_{\alpha\beta}^0$ ,  $g_{\tau\tau}^0 = 0$ ,  $K_{\alpha\alpha}^{\text{O}_2} = K_{\alpha\beta}^{\text{O}_2}$ ). (e) It is noteworthy that the quality of the fit deteriorates, if one introduces additionally the  $\tau\tau$ -interaction-energy as free parameter. Therefore we conclude that the nearest neighbor interaction does not contribute to the allosteric coupling in hemoglobin trout IV.

The obtained values of the free parameters are listed in Table 2. (It should be noted, that the subunits related to

TABLE 2 Equilibrium constants of the  $\text{O}_2$ -binding to hemoglobin trout.

Conformational energies			
Energy type	Parameter value	Error I	Error II
<i>KJ/mol</i>			
$G_{\alpha}^0$	1.4	$\pm 0.3$	$\pm 0.3$
$g_{\alpha}^0$	8.9	$\pm 0.4$	
$g_{\beta}^0$	8.9	$\pm 0.4$	
$G_{\alpha\alpha}^0$	<RT		
$G_{\alpha\beta}^0$	17.9	$\pm 0.4$	
$\text{O}_2$ - affinity			
Constant	Parameter value	Error I	Error II
<i>mmHg-1</i>			
$K_{\alpha\alpha}^{\text{O}_2}$	$3.5 \cdot 10^{-4}$	$\pm 5 \cdot 10^{-8}$	$\pm 10^{-4}$
$K_{\alpha\beta}^{\text{O}_2}$	$3.5 \cdot 10^{-4}$	$\pm 5 \cdot 10^{-5}$	$\pm 10^{-4}$
$K_{\alpha}^{\text{O}_2}$	74.9	$\pm 5$	$\pm 10$
$K_{\beta}^{\text{O}_2}$	74.9	$\pm 5$	$\pm 10$
pK-values of the effector binding sites			
Tertiary effector pK in the unliganded state			
pK-assignment	Parameter value	Error I	Error II
$\text{pK}_{\alpha 1}$	8.5	$\pm 0.1$	$\pm 0.4$
$\text{pK}_{\alpha 2}$	8.5	$\pm 0.1$	$\pm 0.4$
$\text{pK}_{\beta 1}$	7.4	$\pm 0.05$	$\pm 0.1$
$\text{pK}_{\beta 2}$	7.5	$\pm 0.05$	$\pm 0.15$
Tertiary effector pK in the liganded state			
pK-assignment	Parameter value	Error I	Error II
$\text{pK}_{\alpha 1}$	7.1	$\pm 0.15$	$\pm 0.5$
$\text{pK}_{\alpha 2}$	7.6	$\pm 0.1$	$\pm 0.5$
$\text{pK}_{\beta 1}$	6.1	$\pm 0.6$	$\pm 0.9$
$\text{pK}_{\beta 2}$	5.0	$\pm 1.2$	$\pm 1.5$
Quaternary effector sites			
pK-assignment	Parameter value	Error I	Error II
$\text{pK}_{\text{T}_1}$	7.4	$\pm 0.03$	$\pm 0.1$
$\text{pK}_{\text{T}_2}$	7.4	$\pm 0.03$	$\pm 0.1$
$\text{pK}_{\text{R}_1}$	5.4	$\pm 1.2$	$\pm 1.5$
$\text{pK}_{\text{R}_2}$	5.3	$\pm 1.2$	$\pm 1.5$

The standard deviation taken from the on diagonal elements of the inverted Hesse matrix is denoted as error I. Error II results from error analysis carried out with the CONTOUR - plots.

the strong  $q\tau$ -coupling energy are attributed to the  $\beta$ -subunit.) From Table 2C1 and 2C2 one reads that two distinct amino acid residues in the  $\alpha$ - and  $\beta$ -subunits respectively, contribute as tertiary effectors to the Bohr effect. From Table 2C3 one finds two quaternary effector sites which include the Root effect.

In order to check whether other tertiary binding sites have to be considered, we inserted the respective equilibrium constants as additional free parameters into our program. For these parameters, however, the same  $pK$ -values were obtained in both, the oxy- and deoxy form, thus indicating no further contributions to the Bohr effect.

In order to test the validity of the obtained results we have also carried out a fit to CO-binding curves measured at  $T = 5^\circ\text{C}$  by Wyman et al. (1978). All parameters related to the conformation of the molecule in the absence of ligands (conformational free energies,  $pK_L$ ,  $pK_T$ ,  $pK_R$  cf., Table 1) have been taken from Table 2, and are used as fixed parameters in the fit, thus neglecting their temperature dependence. Even though these parameters relate to the unliganded molecule at  $14^\circ\text{C}$ , a good agreement with the experimental data has been obtained from the fitting procedure (Fig. 6). The specific parameters of the CO-liganded states resulting from this fitting procedure are listed in Table 3.

## Error analysis

The program MINUITL contains three different minimizing subroutines named SEEK, SIMPLX, and MIGRAD to search a local minimum of the chi-square function.

The standard deviation of the obtained parameter values were derived by MIGRAD as follows: The routine approximates the chi-square function near to its minimum by a paraboloid centered at the minimum. The

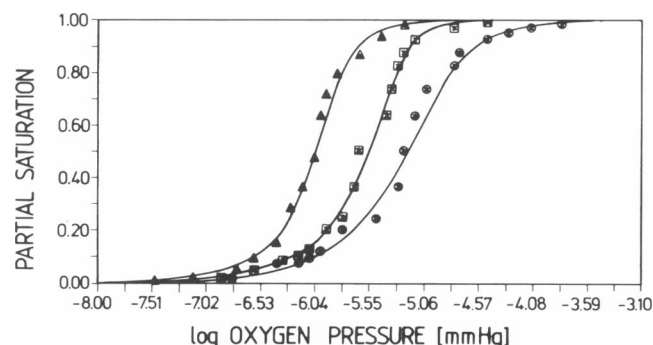


FIGURE 6 Fit to the CO-binding curves of Wyman et al. (1978) carried out by using the conformational energies obtained from the fit to the  $\text{O}_2$ -data set of Brunori et al. (1978).

TABLE 3 Equilibrium constants of the CO-binding to hemoglobin trout IV.

Equilibrium constants of CO – binding			
Constant	Parameter value	Error I	Error II
<i>mmHg<sup>-1</sup></i>			
$K_{L_1}^{\text{CO}}$	$2.3 \cdot 10^4$	$\pm 5 \cdot 10^3$	$\pm 10^4$
$K_{L_2}^{\text{CO}}$	$2.3 \cdot 10^4$	$\pm 5 \cdot 10^3$	$\pm 10^4$
$K_{T_1}^{\text{CO}}$	$7.5 \cdot 10^8$	$\pm 5 \cdot 10^7$	$\pm 10^8$
$K_{T_2}^{\text{CO}}$	$7.5 \cdot 10^8$	$\pm 5 \cdot 10^7$	$\pm 10^8$
Tertiary effector $pK$ in the liganded state			
$pK$ -assignment	Parameter value	Error I	Error II
$pK_{r_{a1}}$	7.7	$\pm 0.1$	$\pm 0.4$
$pK_{r_{a2}}$	8.1	$\pm 0.01$	$\pm 0.4$
$pK_{r_{b1}}$	7.0	$\pm 0.05$	$\pm 0.3$
$pK_{r_{b2}}$	6.5	$\pm 0.1$	$\pm 0.15$

The standard deviation taken from the on diagonal elements of the inverted Hesse matrix is denoted as error I. Error II results from error analysis carried out with the CONTOUR – plots.

standard deviation is provided by the square root of the on diagonal trace elements of the inverted Hesse matrix derived at the minimum. The results of this calculation are listed as error I in the Tables 2 and 3.

The model to be fitted is not linear. Hence the chi-square function may not be approximated reasonably by the paraboloid as described above. In this case the standard deviations calculated from the parabolic approximation do not represent the real statistical error. This was evaluated by the MINUITL subroutine CONTOUR which calculates the projection of the chi-square function on a two dimensional subspace of the parameter space from which the statistical errors are derived. These may be different from those obtained from the Hesse matrix of the symmetric paraboloid.

We have applied the CONTOUR-routine to all parameters which exhibit a high degree of correlation among each other. The degree of correlation can be obtained from the off diagonal elements of the inversed Hesse matrix.

It should be noted, that the application of this procedure yields comparatively large errors for the  $pK_{r_{a1}}$ -,  $pK_{r_{a2}}$ -,  $pK_{r_{b1}}$ - and the  $pK_{R_2}$ -values obtained from the  $\text{O}_2$ -binding curves (cf., error II column in Table 2). Obviously this is due to the fact that the molecule switches from R to T upon approaching the acid pH-region. This causes very small mole fractions of the subunits to be in the high affinity  $r$ -state. Therefore  $r$ -state protonation processes occurring in this pH-region do not influence significantly the effective ligand affinity of the molecule. Thus the binding curves also are only slightly depended on  $pK_r$  and  $pK_R$ .

The errors obtained for the other parameters are



significantly smaller (10–25%, cf., error II-column in Tables 2 and 3). This corroborates the validity of the employed model.

It should be finally noted that the experimental error of the data taken from Brunori et al. (1978) and Wyman et al. (1978) do not contribute significantly to the experimental error.

## DISCUSSION

### Interpretation of the Root effect

The pH-induced shift of the oxygen binding curve is caused by both, tertiary effector binding, which affects directly oxygen binding to the  $\alpha$ - and  $\beta$ -subunits respectively, and quaternary effector binding which increases the effective quaternary energy  $\hat{G}_q^0$  (pH) of Eq. 13. As is displayed in Fig. 7,  $\hat{G}_q^0$  (pH) increases from 1.5 KJ/Mol to nearly 28 KJ/Mol upon approaching the acid pH-region below pH = 6.5.

The influence of this drastic change in cooperativity energy on the binding properties of trout IV is shown in Fig. 8. It depicts the pH-dependence of the allosteric constants  $L_{n_\alpha n_\beta}$  defined by

$$L_{n_\alpha n_\beta} = \frac{[T(n_\alpha^{0_2}, n_\beta^{0_2})]}{[R(n_\alpha^{0_2}, n_\beta^{0_2})]} \quad (31)$$

$[T(n_\alpha^{0_2}, n_\beta^{0_2})]$  represents the concentration of molecules in the quaternary  $T$ -state and  $[R(n_\alpha^{0_2}, n_\beta^{0_2})]$  the concentration of molecules in the  $R$ -state.  $n_\alpha$ ,  $n_\beta$  denote the oxygen occupation of the corresponding  $\alpha$ - and  $\beta$ -subunits, respectively.

The following aspects of the Root-effect can be obtained from this representation: (a) The allosteric constant  $L_{22}$  of the fully liganded molecule is small above pH = 7.0, thus indicating to a predominance of the high affinity  $R$ -state. At pH = 6.6 both types of quaternary

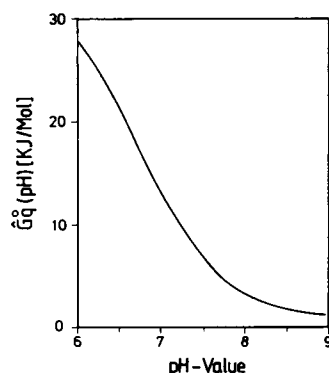


FIGURE 7 pH-dependence of the effective quaternary energy  $\hat{G}_q^0$ (pH).

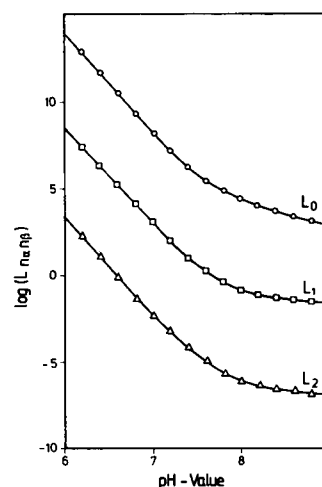


FIGURE 8 pH-dependence of the allosteric constants  $L_{n_\alpha n_\beta}$  ( $n_j$  denotes the occupation-number of the ligand binding sites)

(Circle:  $L_{0,0\beta} = L_{1,0\beta} = L_{2,0\beta} = L_0$   
Diamond:  $L_{0,1\beta} = L_{1,1\beta} = L_{2,1\beta} = L_1$   
Triangle:  $L_{0,2\beta} = L_{1,2\beta} = L_{2,2\beta} = L_2$ )

states are present. Below pH = 6.6, the molecule is predominantly in the low affinity  $T$ -state. (b) The corresponding constant  $L_{00}$  of the unliganded molecule is larger than 100, thus reflecting predominance of the  $T$ -state. (c) An interesting fact is that  $L_{0,0\beta}$ ,  $L_{1,0\beta}$ , and  $L_{2,0\beta}$  become equal. The same is true for the constants  $L_{0,1\beta}$ ,  $L_{1,1\beta}$ , and  $L_{2,1\beta}$ . This shows that lowering of the allosteric constant  $L$  upon oxygen binding is exclusively achieved by binding to the  $\beta$ -subunits because they are affected by  $q\tau$ -interaction. This means that the  $t \rightarrow r$ -transition induced by oxygenation of the  $\alpha$ -subunit does not affect the equilibrium among the quaternary states. Therefore, binding of oxygen molecules to  $\beta$ -subunits is exclusively responsible for the quaternary transitions at a distinct pH-value.

Even though the quaternary effector binding causes a significant decrease of the cooperativity due to an increase of the quaternary energy  $\hat{G}_q^0$ (pH), it does not account for negative cooperativity. As one can learn from our results the asymmetry of the  $q\tau$ -interactions and the different affinity for oxygen binding to the  $\alpha$ - and  $\beta$ -subunits must be considered to explain the binding curves at acid pH-values. The latter effect has been found to be caused by the difference between proton binding to the  $\alpha$ - and  $\beta$ -subunits in accordance with earlier predictions (Brunori, 1975), the pK-values of the  $\beta$ -subunit exhibit a comparatively large shift from pK = 7.5 to 5.8, whereas the pK-changes in the  $\alpha$ -subunits (8.5 to 7.6 and 8.5 to 7.0) do not cause acid pK-values. A slight difference among the equilibrium constants  $K_{i,\alpha}^{0_2}$ ,  $K_{i,\beta}^{0_2}$  and  $K_{i,\alpha}^{0_1}$ ,

$K_{r_s}^0$ , respectively may also be considered, but cannot unambiguously be established, because a good fit can also be obtained without assuming differences in the binding constants.

In contrast to the properties of O<sub>2</sub>-binding, the CO-binding curves at acid pH do not exhibit negative cooperativity. Furthermore, the asymmetry of the binding curves is less pronounced than in the case of O<sub>2</sub>-binding. Due to our analysis this is related to the smaller pK-shift of the involved tertiary effector binding sites upon CO-binding (cf. Table 3). Thus, we can establish a significant difference between the structural changes induced by CO- and O<sub>2</sub>-binding.

## Comparison with other results

It is interesting to check whether the results of our calculations are in accordance with thermodynamic data derived from experiments carried out on Hb-trout IV CO by Wyman et al. (1978) comprising microcalorimetric and binding studies. Using these data Ascoli et al. (1986) determined the energy difference among the fully liganded and unliganded *T*- and *R*-states for pH = 6.0, respectively with CO as ligand. The respective values are listed in Table 4.

The same quantities can be derived from the results of our analysis in the following way: First one calculates the occupation probability *P* of all molecular states at different CO-pressure and pH-values by using the equation

$$P_{q,n_j,\tau_j} = \frac{\exp \left\{ - \sum_j [-n_j \mu_L + G_{\text{eff}}(\tau_j, q, \text{pH})] / RT \right\}}{Z}, \quad (32)$$

where  $G_{\text{eff}}(\tau_j, q, \text{pH})$  denotes the total effective energy of the actual conformational state and  $n_j$  is the ligand occupation number of the *j*th subunit.

This yields for pH = 6.0 that for each  $P_{\text{CO}}$ -value the {*T*, 4*t*} and {*R*, 2*t*, 2*r*} is by far the predominant conformation in the fully liganded state, whereas the {*T*, 2*r*, 2*t*}

and {*R*, 4*r*} conformations dominate in the unliganded state. The concentrations of all other conformations are several orders of magnitude smaller and are neglected.

The respective energy difference among the *T<sub>u</sub>*, *R<sub>u</sub>*, *T<sub>L</sub>*, and *R<sub>L</sub>* (*u*: unliganded, *L*: fully liganded) can therefore be calculated by using the equations:

$$\Delta G(T_u \rightarrow R_u) = RT \ln \left\{ \frac{[T_u]}{[R_u]} \right\} = \hat{G}_q^0(\text{pH} = 6.0) + 2g_{r_s}^0 + 2G_{q_{r_a}}^0 \quad (33)$$

$$\Delta G(T_L \rightarrow R_L) = RT \ln \left\{ \frac{[T_L]}{[R_L]} \right\} = \hat{G}_q^0(\text{pH} = 6.0) + 2g_{r_s}^0 + 2G_{q_{r_a}}^0 - 2RT \{ \ln K_{r_s}^{\text{co}} - \ln K_{r_s}^{\text{co}} \} \quad (34)$$

$$\Delta G(T_u \rightarrow T_L) = RT \ln \left\{ \frac{[T_L]}{[T_u] P_{\text{CO}}^4} \right\} = 2g_{r_s}^0 + 2G_{q_{r_a}}^0 - 2RT \{ \ln K_{r_s}^{\text{co}} - \ln K_{r_s}^{\text{co}} \} + 2RT \left\{ \sum_j (pK_{r_j} - pK_{t_j}) \right\} \quad (35)$$

$$\Delta G(R_u \rightarrow R_L) = RT \ln \left\{ \frac{[R_L]}{[R_u] P_{\text{CO}}^4} \right\} = -\Delta G(T_u \rightarrow R_u) + \Delta G(T_u \rightarrow T_L) + \Delta G(T_L \rightarrow R_L). \quad (36)$$

Table 4 lists the values obtained from these calculations. If one considers that the data of Wyman et al. (1978) also result from a model dependent fit to their experimental results, the agreement between both data sets is convincing.

## Effector binding

Perutz and Brunori (1982) suggested a stereochemical interpretation of the Root effect, which is based on the knowledge of the primary structure of some fish hemoglobin systems displaying this effect. They focussed their interest on F9β-position, occupied by a cysteine in human hemoglobin, and replaced by serine in all considered fish hemoglobin systems. Because of the hydrophobic character of serine it is likely to prefer a position similar to the external one of CysF9β in human hemoglobin (cf., Shaan, 1983). Due to Brunori and Perutz this enables the OH of serine to donate an H-bond to the terminal oxygen of His(HC3)β and accept a hydrogen from the peptide NH of His(HC3)β in the *T*-structure. Those bonds would stabilize the C-terminal saltbridges and enable the imidazole of His(HC2)β to form a saltbridge with Glu(FG6).

TABLE 4 Energy difference among the unliganded and liganded *T*- and *R*-state of HbCO-trout IV.

	Wyman et al. parameter values	Our parameter values
$G(T_u \rightarrow R_u)$	39. kJ/mol	44 kJ/mol
$G(T_L \rightarrow R_L)$	-3.7 kJ/mol	-4.1 kJ/mol
$G(T_u \rightarrow T_L)$	-107 kJ/mol	-116 kJ/mol
$G(R_u \rightarrow R_L)$	-150 kJ/mol	-164 kJ/mol

Information obtained from experiments by Wyman et al. (1978) and from our calculations.

This imposes a constraint on the functional important FG-helix, which can be expected to influence both, the functional heme group (Wedekind et al., 1985) and the  $\alpha\beta$  contacts (Baldwin and Chothia, 1979). It has been shown that this provides an important contribution to cooperativity.

In order to account for the pH-dependence of cooperativity in Hb-trout IV we have considered two quaternary effector binding sites to exist. The pK-values for effector 1 are 7.4 and 5.1 in the *T*- and *R*-state, respectively. For effector 2 one finds 7.4 and 5.4 correspondingly (Table 3). If the model of Perutz and Brunori is even partially valid, one of these pK's has to be assigned to His(HC2) $\beta$ . It is difficult to imagine, however, that the pK of imidazole is lower than 6.0. Therefore, it is reasonable to assume that other amino acid groups contribute to the Root-effect, and that the obtained pK-shifts have to be interpreted as effective values. Further investigations are necessary to clarify this point.

The Root effect is superimposed by the Bohr effect, which has been found to be different for O<sub>2</sub>- and CO-binding. Therefore, one can conclude that the related effector binding affects directly the ligand affinity as it is described by our theory.

As one can read from Table 2, for each subunit ( $\alpha$  or  $\beta$ ) two amino acid groups contribute to the Bohr effect. For the  $\alpha$ -subunit one obtains pK-shifts from 8.5 to 7.0 and 8.5 to 7.6, thus providing free energy in the alkaline region. For the  $\beta$ -chain, one obtains pK-shifts from 7.5 to 5.8 and 7.4 to 5.9, which covers also the region of the Root effect. In the case of CO-binding, the Bohr effect is less pronounced. For the  $\alpha$ -chains we obtained 8.5 to 8.1 and 8.5 to 7.7, in the  $\beta$ -chain 7.4 to 7.0 and 7.5 to 6.0, respectively.

It is not possible to relate these pK-values to distinct amino acid side chains, even though it may be reasonable to assume that the pK-shifts assigned to the  $\beta$ -chains, i.e., 7.5 to 5.8 for O<sub>2</sub>- and 7.5 to 6.0 for CO-binding, can be attributed to His(HC3) $\beta$ . Further investigations, for instance theoretical analysis of the ligand binding to modified trout IV-hemoglobin, is necessary to clarify this point.

This work is supported by a grant of the Deutsche Forschungsgemeinschaft.

We would like to thank Mr. Ankele for drawing the figures and Mrs. Niemeyer for typing the manuscript.

Received for publication 13 May 1988 and in final form 1 November 1988.

## REFERENCES

- Ascoli, T., G. Falcioni, B. Giardina, and M. Brunori. 1986. Thermodynamic characterization of the allosteric transition in trout hemoglobin. *Eur. Biophys. J.* 13:245-249.
- Baldwin, J. L., and C. Chothia. 1979. Haemoglobin, the structure changes related to ligand binding and its allosteric mechanism. *J. Mol. Biol.* 129:175-200.
- Brunori, M. 1975. Molecular adaption to physiological requirements. *Curr. Top. Cell. Regul.* 9:1-39.
- Brunori, M., M. Coletta, B. Giardina, and J. Wyman. 1978. A macromolecular transducer as illustrated by trout hemoglobin IV. *Proc. Natl. Acad. Sci. USA.* 75:4310-4312.
- Herzfeld, J., and E. Stanley. 1974. A general approach to cooperativity and its application to the oxygen equilibrium of hemoglobin and its effectors. *J. Mol. Biol.* 82:231-265.
- James, F. 1972. Function minimization. Proceedings of the 1972 CERN-computing and Data Processing School, Pertisau/Austria, Cern. 72-21.
- Koshland, D. E., G. Nemethy, and D. Filmer. 1966. Comparison of experimental binding data and theoretical models in proteins containing subunits. *Biochemistry.* 5:365-385.
- Monod, J., J. Wyman, and J. P. C. Changeaux. 1965. On the nature of allosteric transitions: a sensible model. *J. Mol. Biol.* 12:88-118.
- Perutz, M. F. 1970. Stereochemistry of cooperative effects in haemoglobin. *Nature (Lond.)*. 228:726-734.
- Perutz, M. F., and M. Brunori. 1982. Stereochemistry of cooperative effects in fish and amphibian haemoglobin. *Nature (Lond.)*. 299:421-426.
- Shaanan, B. 1983. Structure of human oxyhemoglobin at 2:1 Å resolution. *J. Mol. Biol.* 171:31-59.
- Schweitzer-Stenner, R., D. Wedekind, and W. Dreybrodt. 1989. Allosteric transitions in oxyHb trout IV detected by resonance Raman spectroscopy. *Biophys. J.* 55:703-712.
- Szabo, A., and M. Karplus. 1972. A Mathematical model for structure-function relations in hemoglobin. *J. Mol. Biol.* 72:163-197.
- TenEyck, L. F. 1979. Hemoglobin and Myoglobin. In *The Porphyrins* Vol. III, D. Dolphin, editor. Academic Press Inc., New York.
- Wyman, J., S. J. Gill, H. T. Gaud, A. Colosimo, B. Giardina, H. A. Kuiper, and M. Brunori. 1978. Thermodynamics of ligand binding and allosteric transition in hemoglobins. Reaction of Hb trout IV with CO. *J. Mol. Biol.* 124:161-175.
- Wedekind, D., R. Schweitzer-Stenner, and W. Dreybrodt. 1985. Heme-apoprotein interaction in the modified oxyhemoglobin-bis(N-maleimidoethyl)ether and in oxyhemoglobin at high Cl<sup>-</sup>-concentration denoted by resonance Raman scattering. *Biochim. Biophys. Acta.* 830:224-232.